Geol Rundsch (1994) 83: 502–513

A. Kröner · J. Krüger · A. A. A. Rashwan

Age and tectonic setting of granitoid gneisses in the Eastern Desert of Egypt and south-west Sinai

Received: 18 November 1993 / Accepted: 15 April 1994

Abstract Strongly deformed and locally migmatized gneisses occur at several places in the southern Eastern Desert of Egypt and in Sinai and have variously been interpreted as a basement to Pan-african (≈900 to 600 Ma) supracrustal and intrusive assemblages. A suite of grabbroic to granitic gneisses was investigated in the Hafafit area, which constitutes an I-type calc-alkaline intrusive assemblage whose chemistry suggests emplacement along an active continental margin and whose granitoid members can be correlated with the so-called 'Older Granites' of Egypt. $^{207}Pb/^{206}Pb$ single zircon evaporation from three samples of the Hafafit gneisses yielded protolith emplacement ages between 677 ± 9 and 700 ± 12 Ma and document granitoid activity over a period of about 23 Ma. A migmatitic granitic gneiss from Wadi Bitan, south-west of Ras Banas, has a zircon age of 704 ± 8 Ma, and its protolith was apparently generated during the same intrusive event as the granitoids at Hafafit. Single zircons from a dioritic gneiss from Wadi Feiran in south-west Sinai suggest emplacement of the protolith at 796 ± 6 Ma and this is comparable with ages for granitoids in north-east Sinai and southern Israel. None of the above gneisses is derived from remelting of older continental crust, but they are interpreted as reflecting subduction-related calc-alkaline magmatism during early Pan-african magmatic arc formation.

Key words Eastern Desert, Egypt · Granitoid gneisses · Single zircon dating

A. Kröner ✉ · J. Krüger[1]
Institut für Geowissenschaften, Universität Mainz,
D-55099 Mainz, Germany
Fax (06131) 39 47 69

A. Abdelazeem Ahmed Rashwan
Egyptian Geological Survey and Mining Authority,
3 Salah Salem Street, Abbasiya, Cairo, Egypt

Present address:
[1] Warmsrother Grund 11,
D-55442 Stromberg

Introduction

There is still considerable controversy about the tectonic position and age of granitoid gneisses in the Eastern Desert (ED) of Egypt and in Sinai. These occur in antiformal, 'domal' positions, generally surrounded by lower grade supracrustal assemblages (see summary in Greiling et al., 1994). In the ED such rocks occur at Meatiq (Sturchio et al., 1983; 1984; El-Gaby et al., 1984; Habib et al., 1985; Bennet and Mosley 1987), in three distinct domal structures at Hafafit (Greiling and El-Ramly, 1990; Rashwan, 1991) and in the region along Wadis Bitan and Haimut (Geological Map 1:500 000, sheet NF 36 NE Bernice, Technische Fachhochschule Berlin 1987). In south-western Sinai similar rocks occur in the Wadi Feiran region (El-Gaby and Ahmed, 1980; Shimron, 1980). Schürmann (1966), El Ramly and Akaad (1960) and El Ramly (1972) considered these gneisses to form a basement onto which a 'geosynclinal assemblage' of metasediments and metavolcanic rocks was deposited. They also separated these rocks from less deformed, variably foliated granitoids which are known as 'Grey' or 'Older' Granitoids (El Ramly and Akaad, 1960; Hussein et al., 1982) and also include the so-called 'Metagabbro-Diorite Complex' (Geological Map of Egypt, 1981). Sturchio et al. (1983; 1984) were the first to document, from detailed work at the Meatiq dome, that the gneisses there do not constitute a basement but acquired their relatively high metamorphic grade in the Late Proterozoic during the Pan-African event.

El Ramly et al. (1984) and Greiling et al. (1984; 1988) reinvestigated the tectonic relationships in the Hafafit area and interpreted the gneisses as syntectonic granitoid intrusives during the formation of an Andean-type continental margin, which were subsequently deformed during a period of thrust stacking. Kröner et al. (1987) considered these rocks to constitute a genetically related suite of I-type granitoids, similar to those found in the Late Precambrian (Pan-African) island-arc environment of the Arabian Shield and in modern magmatic arcs, and they

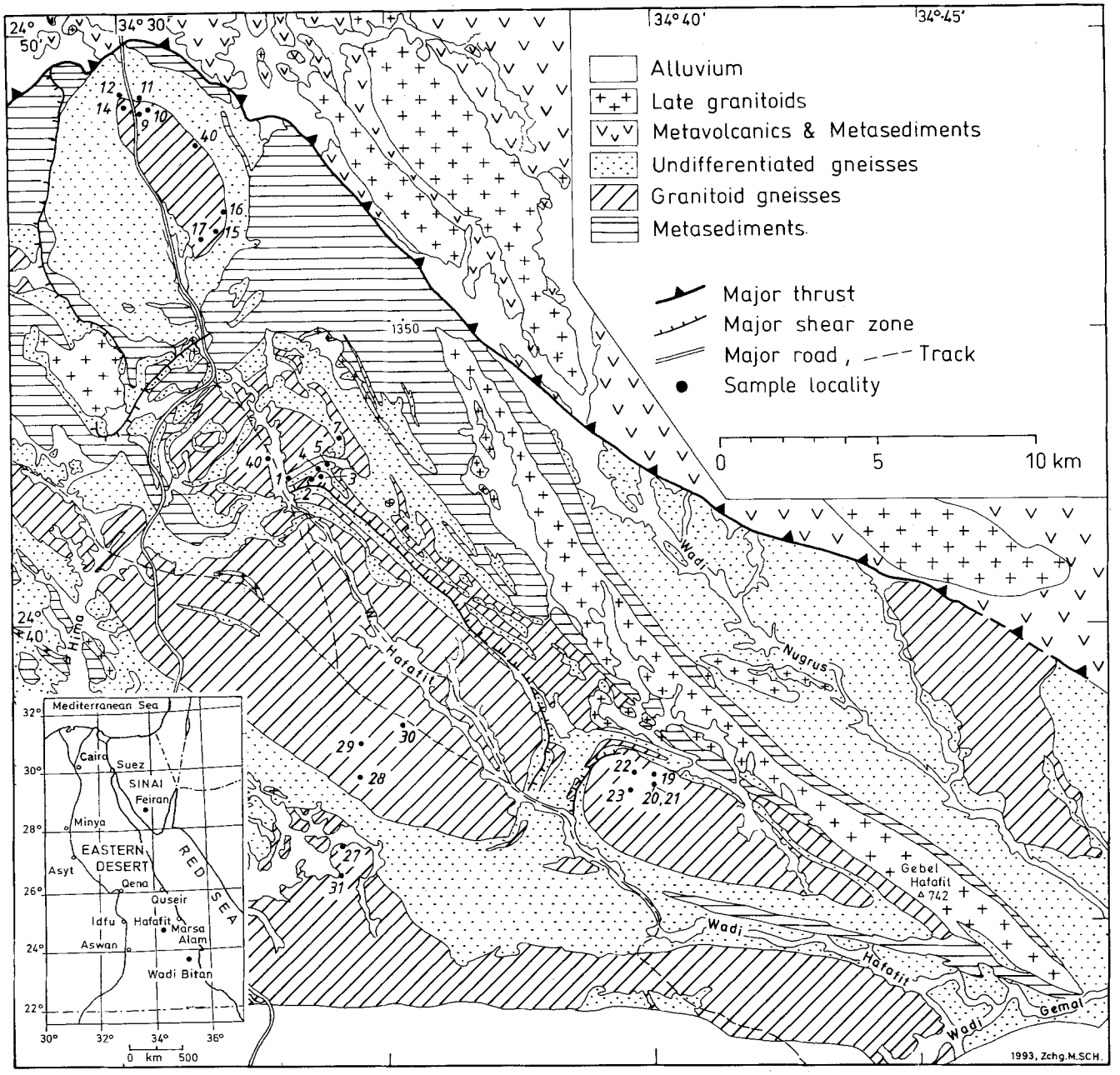

Fig. 1. Simplified geological map of the Wadi Hafafit area showing major rock types, structures and sample localities. Based on map by Greiling and El Ramly (1990)

also suggested that these rocks are part of the 'Older Granite' (El Ramly and Roufaiel, 1974; Hussein et al., 1982) suite of intrusives. In this view, the gneisses were originally emplaced as plutonic rocks during early deformation of the supracrustal assemblage about 680–710 Ma ago and during the onset of thrust tectonics (Kröner et al., 1987).

In contrast, El-Gaby et al. (1984; 1988; 1990) considered all the above granitoid gneisses as extensions of Mid-Proterozoic crust as exposed in the Western Desert of Egypt (Harris et al., 1984; 1990; Schandelmeier et al., 1988), also known as the East Saharan Craton (Kröner, 1979; Schandelmeier et al., 1988). In this view the gneisses constitute a basement onto which the Pan-African supracrustal assemblage was deposited and which was subsequently deformed and metamorphosed together with this cover, resulting in migmatites and 'remobilized infrastructural rocks' (El-Gaby et al., 1988). These workers did not provide convincing field or other evidence for their view but cited a $^{207}Pb/^{206}Pb$ age of 1770 Ma obtained by Abdel-Monem and Hurley (1979) on one zircon fraction from a gneissose granite in Wadi Sikait east of Hafafit. Kröner et al. (1988) have discussed this age and interpreted the data of Abdel-Monem and Hurley (1979) as reflecting granite emplacement at about 780 Ma, with the anomalously old fraction representing a mixture of zircon grains of predominantly xenocrystic origin. They

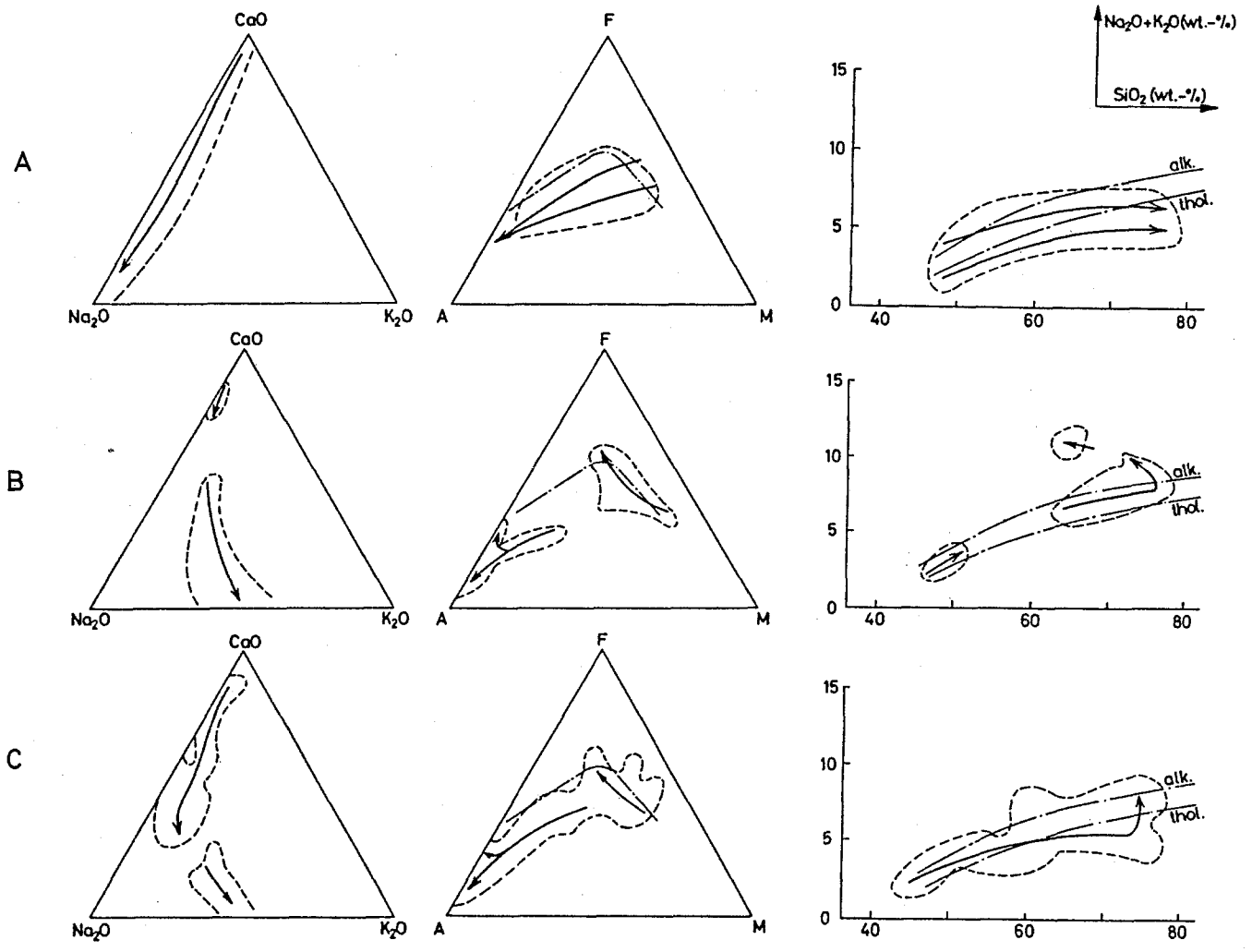

Fig. 2 A–C. Ternary $Na_2O-CaO-K_2O$, AFM and alkali silica diagrams summarizing the chemical evolution of magmatic rocks in the Arabian shield (A and B) and in the Hafafit area, southeastern Desert of Egypt (from Kröner et al., 1987). **A** Mantle-derived and subduction-related 'primary crust' (andesitic assemblage and dioritic suite; Schmidt and Brown, 1984). **B** Associations produced after collision and cratonization (rhyolitic assemblage and granite gabbro suite, Schmidt and Brown, 1984). **C** Calc-alkaline magmatic association, Hafafit area (present data and J. Krüger, unpublished data)

also discussed other age data apparently indicating a pre-Pan-African (i.e. >950 Ma) crustal element in the ED, but concluded that these data are either unreliable or imprecise so that there is as yet no conclusive evidence for the existence of Early to Mid-Proterozoic rocks in the ED east of the River Nile. The Wadi Feiran gneisses of south-west Sinai were also considered to be of pre-Pan-African age (Schürmann, 1966; Shimron, 1980), but Stern and Manton (1987) have shown convincingly on the basis of Sr isotopes and a zircon age that these rocks cannot be older than ≈780 Ma.

Isotopic dating of the disputed gneisses at Hafafit and in the southern ED is so far restricted to one zircon age for a migmatized and foliated tonalite sample in the core of the Migif-Hafafit Dome (location, see Fig. 1 and Greiling and El Ramly, 1990) that yielded a U–Pb age of 682 Ma (error not given) and an initial $^{87}Sr/^{86}Sr$ ratio of 0.7024 (Stern and Hedge, 1985). The Sr initial ratio alone precludes derivation of this rock from an Early to Mid-Proterozoic source and reiterates the conclusions of Kröner et al. (1987) about the origin of this rock. Tonalitic plutons of the 'Older Granite' suite south of Hafafit yielded U–Pb zircon ages of ≈710 Ma and low $^{87}Sr/^{86}Sr$ ratios of 0.7024–0.7025 (Dixon, 1981; Stern and Hedge, 1985), comparable with the data for the above gneiss from Hafafit. Two samples of the 'Shaitian Granite' (El Kaliuobi and El Ramly 1991), equivalent to the Older Granite suite in the terminology of El Ramly and Roufaiel (1974), from an occurrence north-west of the Hafafit Culmination yielded U–Pb and Pb–Pb zircon ages around 730 Ma (Stern, Greiling and Kröner, unpublished data). About 710 Ma old orthogneisses are found in a nearly continuous strip extending from the southern ED into the Red Sea Hills north-eastern Sudan (Stern et al., 1989; Stern and Kröner, 1993).

We have chemically analysed a variety of variably deformed plutonic rocks from the two northern domal culminations at Hafafit (Fig. 1), ranging from gabbro to leucogranite in composition, and we also dated two samples of the suite from the largest gneiss culmination

Table 1. Chemical composition (in weight %), selected major element ratios and trace element concentrations (in ppm) for gabbroic to granitic rocks of the Hafafit area, Egypt (J. Krüger, unpublished data)

	EG 1	EG 2	EG 3	EG 4	EG 5	EG 7	EG 9	EG 10	EG 11
SiO_2	53.71	53.93	54.09	53.54	55.31	58.48	76.74	58.92	59.00
TiO_2	0.44	0.47	0.47	0.88	0.47	0.36	0.34	0.50	0.47
Al_2O_3	17.32	16.49	16.11	15.79	15.93	13.79	1.80	21.06	15.77
Fe_2O_3	5.12	3.33	3.26	3.74	3.76	3.03	1.37	2.01	3.14
FeO	1.61	3.43	3.97	4.46	5.36	4.37	0.86	1.93	4.63
MnO	0.16	0.16	0.17	0.18	0.19	0.14	0.04	0.09	0.18
MgO	6.63	6.72	7.43	7.03	4.08	4.53	0.53	1.75	3.25
CaO	9.80	9.99	9.92	9.34	9.08	10.05	2.63	5.71	7.44
Na_2O	0.36	3.10	3.04	3.06	3.25	2.62	3.81	5.65	3.68
K_2O	0.37	0.27	0.18	0.33	0.94	0.52	0.90	1.56	0.80
P_2O_5	0.06	0.06	0.06	0.13	0.13	0.09	0.04	0.09	0.15
H_2O^+	0.84	1.43	1.38	1.31	1.41	1.28	0.55	1.00	1.30
H_2O^-	0.11	0.18	0.18	0.11	0.08	0.09	0.00	0.00	0.10
CO_2	0.10	0.02	0.01	0.02	0.06	0.60	0.01	0.02	0.12
Total	99.63	99.58	100.27	99.92	100.05	99.95	99.62	100.29	100.03
K_2O/Na_2O	1.1	0.09	0.06	0.11	0.29	0.20	0.24	0.28	0.22
$K_2O + Na_2O$	3.73	3.37	3.22	3.39	4.19	3.14	4.71	7.21	4.49
FeO/Fe_2O_3	0.31	1.03	1.22	1.19	1.43	1.44	0.63	0.96	1.48
Ba	92.0	77	69	63	108	74	233	390	101
Nb	2.2	1.8	2.5	3.6	3.0	2.2	4.25	6.15	2.45
Zr	57.0	64	60	118	28	38	94.6	80.2	31.3
Y	11.7	13.0	12.3	17.6	17	14.7	29.3	30.7	18.7
Sr	447	449	430	329	196	167	226	444	261
Rb	3.2	6.15	3.9	4.25	6.45	5.25	21.7	34.3	5.05
Zn	651	649	669	715	770	686	446	546	706.0
Cu	1063	1138	1149	1137	1311	1199	797	1818	1245.0
Ni	65	54	59	68	24	33	–	7.5	10.5
Co	28	30	32	34	36	27	12	38	64.5
Cr	95	99	101	226	27	102	3.5	11.0	21.5
V	97	111	109	144	288	250	35.5	70.5	227.0

Tabelle 1. (Continued)

	EG 12	EG 14	EG 15	EG 16	EG 17	EG 19	EG 20	EG 21
SiO_2	62.30	75.40	67.38	73.10	60.10	75.38	69.55	69.40
TiO_2	0.36	0.36	0.42	0.46	0.95	0.35	0.56	0.32
Al_2O_3	14.25	11.93	16.75	13.32	16.82	13.08	14.13	15.89
Fe_2O_3	2.64	1.64	1.12	1.54	2.50	1.69	3.03	1.79
FeO	4.61	1.16	1.16	1.34	2.63	1.14	1.68	0.86
MnO	0.14	0.06	0.05	0.06	0.08	0.06	0.06	0.06
MgO	3.43	0.60	1.34	0.71	2.89	0.69	0.82	0.93
CaO	7.31	3.21	4.44	3.09	5.80	2.28	3.18	0.81
Na_2O	3.06	3.55	4.66	4.97	4.06	4.03	4.27	4.60
K_2O	0.84	0.64	1.29	1.20	1.55	1.05	1.24	1.07
P_2O_5	0.05	0.07	0.12	0.08	0.32	0.10	0.19	0.11
H_2O^+	1.23	0.45	0.69	0.52	1.06	0.82	0.66	0.96
H_2O^-	0.09	0.00	0.00	0.00	0.08	0.12	0.00	0.08
CO_2	0.10	0.01	0.02	0.05	0.19	0.21	0.08	0.00
Total	100.41	99.07	99.44	100.44	99.03	101.00	99.45	99.88
K_2O/Na_2O	0.27	0.18	0.28	0.30	0.38	0.26	0.29	0.23
$K_2O + Na_2O$	3.90	4.19	5.94	5.17	5.61	5.08	5.51	5.66
FeO/Fe_2O_3	1.75	0.71	1.04	0.87	1.05	0.68	0.55	0.48
Ba	106	153	304	259	306	304	442	288
Nb	2.90	5.05	3.7	5.9	10.6	3.05	3.25	2.65
Zr	37.8	91.8	11.4	305	192	68.4	32	67.5
Y	16.9	45	9.9	15.8	15.9	16.2	20.9	16.5
Sr	170	159	492	280	538	439	377	438
Rb	10.2	13.7	51.4	46.1	36.7	21.1	29.4	21.9
Zn	652	507	521	525	660	565	558	523
Cu	1075	822	861	886	1016	885	908	846
Ni	18	–	4.0	–	18.5	–	–	–
Co	70	120	74.5	95	59	91.5	120	110
Cr	55.5	5.0	14.0	3.5	5.6	6.0	5.0	6.5
V	236	47.5	42.5	13.5	102	42.5	45	41

For continuation of table 1 please see the next page

Tabelle 1. (Continued)

	EG 22	EG 23	EG 27	EG 28	EG 29	EG 30	EG 31	EG 40
SiO_2	72.82	74.62	65.87	65.79	2.18	74.59	71.94	71.00
TiO_2	0.15	0.37	0.36	0.43	0.15	0.14	0.41	0.34
Al_2O_3	15.63	12.82	17.06	16.93	15.13	14.54	15.50	13.81
Fe_2O_3	0.64	1.47	2.36	2.47	0.70	0.68	0.90	1.76
FeO	0.64	1.35	1.08	1.41	0.42	0.33	0.64	1.79
MnO	0.03	0.06	0.08	0.09	0.04	0.07	0.03	0.06
MgO	0.37	0.69	1.36	1.40	0.38	0.37	0.42	1.15
CaO	2.90	2.18	5.13	5.22	3.32	2.67	3.33	3.78
Na_2O	5.48	3.96	4.66	4.53	5.43	5.33	5.31	3.65
K_2O	0.69	1.03	0.78	0.78	0.79	0.84	0.85	1.09
P_2O_5	0.05	0.10	0.14	0.15	0.04	0.03	0.03	0.07
H_2O^+	0.47	0.56	0.45	0.64	1.47	0.37	0.62	0.00
H_2O^-	0.07	0.07	0.00	0.00	0.00	0.00	0.00	0.01
CO_2	0.04	0.06	0.16	0.06	0.00	0.12	0.11	0.00
Total	99.34	99.34	99.49	99.90	100.05	100.08	99.86	98.51
K_2O/Na_2O	0.13	0.26	0.17	0.17	0.15	0.16	0.16	0.30
$K_2O + Na_2O$	6.17	4.98	5.44	5.30	6.22	6.17	6.16	2.48
FeO/Fe_2O_3	1.00	0.92	0.46	0.57	0.60	0.49	0.71	1.02
Ba	211	288	185	186.5	232	276	31	281
Nb	1.45	3.0	2.1	3.0	2.45	2.95	3.55	4.25
Zr	66.8	268	66.1	72.2	55.3	52.60	107	60.6
Y	6.4	22.2	11.6	11.6	6.1	9.35	7.3	17.1
Sr	460	351	437.4	43	435	3.0	431	
Rb	13.3	27.3	11.9	13.0	13.5	10.9	20.5	
Zn	467	492	534	546	445	421	448	
Cu	779	828	870	927	765	744	757	
Ni	–	–	–	2	–	–	–	
Co	91	79	69.5	63.5	94.5	88.5	101	
Cr	5.5	6.0	7.5	9.5	7.0	5.0	2.5	
V	13.5	26.0	49.5	61	13.5	10.5	15.0	

and one from weakly foliated granitoids outside the dome structures using the single zircon evaporation technique. Furthermore, we dated a strongly foliated granitic gneiss from Wadi Bitan in the southern ED (inset, Fig. 1) and a foliated diorite from Wadi Feiran in south-west Sinai (inset, Fig. 1) to place further constraints on the age origin of these rocks.

Regional geology, sample description and geochemistry

Most-samples come from the two northern gneiss culminations at Hafafit and were chemically analysed for major and trace elements to complement the data collection of Rashwan (1991). The data are presented in Table 1 and the sample locations are given in Fig. 1.

The geology and structural evolution of the Hafafit area has been described in some detail by Greiling et al. (1984), Greiling and El Ramly (1990) and Rashwan (1991). The core of four distinct antiformal culminations are composed of strongly foliated gneisses of plutonic origin ranging in composition from gabbro to leucogranite. Ultramafic rocks, now largely serpentinite, occur as tectonic lenses (originally dykes and/or xenoliths) in these gneisses and probably represent the most primitive members of the Hafafit plutonic suite. The mafic varieties occur largely as banded amphibolites or amphibole plagioclase gneisses, whereas the tonalitic to granitic members are represented by leucocratic orthogneisses with variable proportions of hornblende, biotite and K-feldspar (Kröner et al., 1987). Migmatization is most pronounced in the siliceous gneisses.

Intrusive and structural contacts show a temporal relation between these rock types from the oldest ultramafic gabbroic phases to the youngest granodiorite granite varieties. The gabbroic to tonalitic members of the suite largely constitute the outer margins of the dome structures at Hafafit, whereas the leucocratic granitoids make up the cores, but occasionally also occur tectonically interlayered between the other gneisses. The central parts of the domes also contain the least strained, competent rocks whose igneous character is easily recognized and where intrusive contacts are best preserved. Markedly less deformed but distinctly foliated granitoids indistinguishable from those with the domes make up large granitoid terrains to the south-east and south of the Hafafit structures (Therani et al., 1988; Greiling and El-Ramly, 1990) and are classified as 'Older Granitoids' (Geological Map of Egypt, 1981).

Field relationships suggest that the igneous suite at Hafafit was generated during several temporally distinct intrusive episodes during which increasing differentiation led to plutonic bodies ranging from minor ultramafic dykes to voluminous monzogranites. Kröner et al. (1987) demonstrated on the basis of major element relationships

that the Hafafit suite displays a calc-alkaline trend (Fig. 2C), similar to the 'Shaitian granites' (El Kaliuobi and El Ramly, 1991) and granitoid rocks in the Arabian shield (Fig. 2A; Schmidt and Brown, 1984). The Hafafit trends (Fig. 2C) have similarities with those of igneous suites generated during magmatic crustal thickening (underplating) below active continental margins (Barker et al., 1981).

Rashwan (1991) provided detailed petrographic descriptions and chemical analyses of the gabbroic and granitoid gneisses in the northern dome at Hafafit, which are complemented by our present data. These data show the granitoids to range in composition from tonalite to granite. Major constituents are variable proportions of plagioclase (mainly oligoclase), quartz, hornblende, biotite and K-feldspar.

Chemically the Hafafit granitoids are similar to the Shaitian granitoids as documented by El Kaliuobi and El Ramly (1991), and we have no doubt that they are part of this extensive suite of rocks exposed in the central and southern ED and in the Red Sea Hills of north-east Sudan. They are also similar to a suite of calc-alkaline granitoids described from the northern ED by Abdel-Rahman and Martin (1987). In the AFM diagram (Fig. 3) the gabbros and granitoids form a well defined trend in the calc-alkaline field. Rashwan (1991) has shown that the alkalinity index also suggests a calc-alkaline affinity and, on the basis of $Al_2O_3/(CaO + Na_2O + K_2O)$ molar ratios (A/CNK) less than 1.1, our granitoids are metaluminous and of the I-type (Chappell and White, 1974). In the An–Ab–Or ternary diagram the data of Rashwan (1991) cover the fields of tonalite, granodiorite and granite, whereas our additional data indicate abundant trondhjemites, no granodiorites and only two granites (Fig. 4). Thus the entire spectrum of compositions commonly found in calc-alkaline plutonic rocks of island arc complexes is present in the gabbroic and granitoid gneisses at Hafafit.

Trace element data support the island arc setting for these granitoids. Only the two granite samples with $SiO_2 > 72\%$ have Nb contents of 16–20 ppm, whereas the tonalites and trondhjemites have very low Nb values well below 15 ppm, as is typical of granitoids formed above subduction zones (Pearce and Gale, 1977). In terms of the Nb, Y and Rb contents (Fig. 5) the Hafafit granitoids plot in the field of volcanic arc granites of Pearce et al. (1984). Variations in the Zr contents in the gabbros and granitoids correlate with the $(Na_2O + K_2O_3)/Al_2O_3$ ratio, in line with zircon solubility studies of Watson (1979). The abundances of Ba, Sr and Rb are related directly to the proportions of feldspar present. Sr is mainly concentrated in plagioclase, whereas Ba and Rb are preferentially incorporated in K-feldspar and biotite. The Cu and Zn contents are unusually high, but we have no explanation for this phenomenon.

In general, our chemical data in conjunction with the results of Rashwan (1991) support the model of El Ramly et al. (1984), who suggested that the Hafafit granitoids

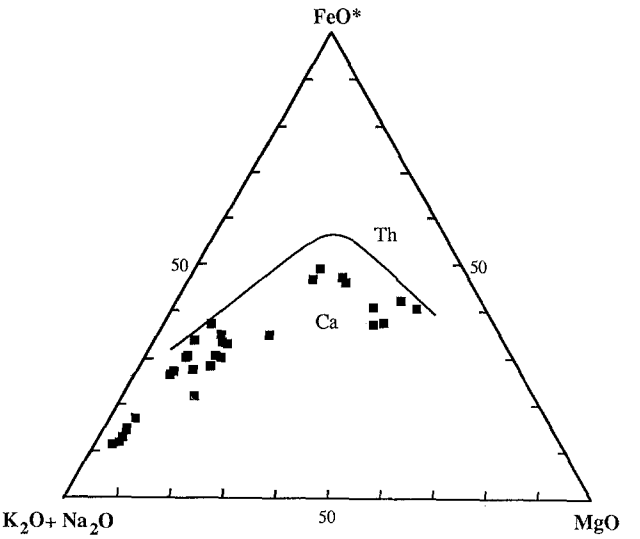

Fig. 3. AFM diagram showing calc-alkaline trend of Hafafit gabbros and granitoids (data from Table 1). Ca calc-alkaline field; Th tholeiitic field

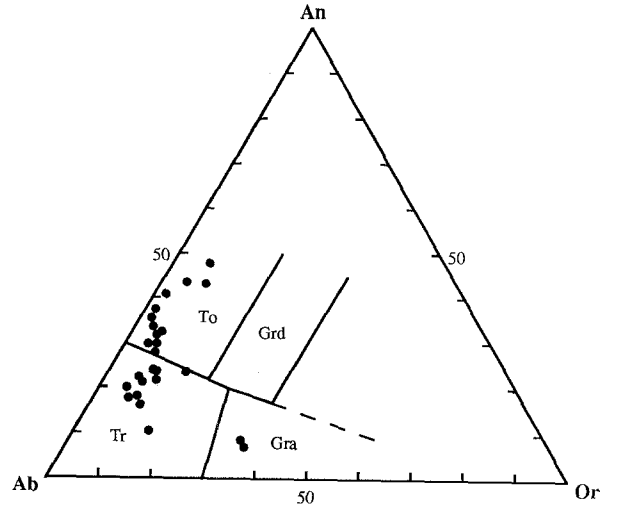

Fig. 4. Normative An–Ab–Or diagram (based on Table 1) showing composition of Hafafit granitoids. To = Tonalite; Tr = trondhjemite; Grd = granodiorite; Gra = granite

formed in an active arc setting at a time when supracrustal rocks, possibly derived from both an emerging arc and a continental margin to the west, began to become deformed.

Samples selected for zircon dating were chosen to represent two distinct rock groups, namely trondhjemite (EG 27 and 28) and granodiorite (EG 30) which, on field evidence, intruded in this order.

The granitoid gneiss terrain in the Wadi Bitan area of the southern ED was described in detail by Stietzel (1987) and Abdel-Khalek et al. (1992). The former workers distinguished between hornblende gneiss, derived from either quartz diorite or andesite, tonalitic to granitic orthogneisses, migmatitic gneisses and amphibolite.

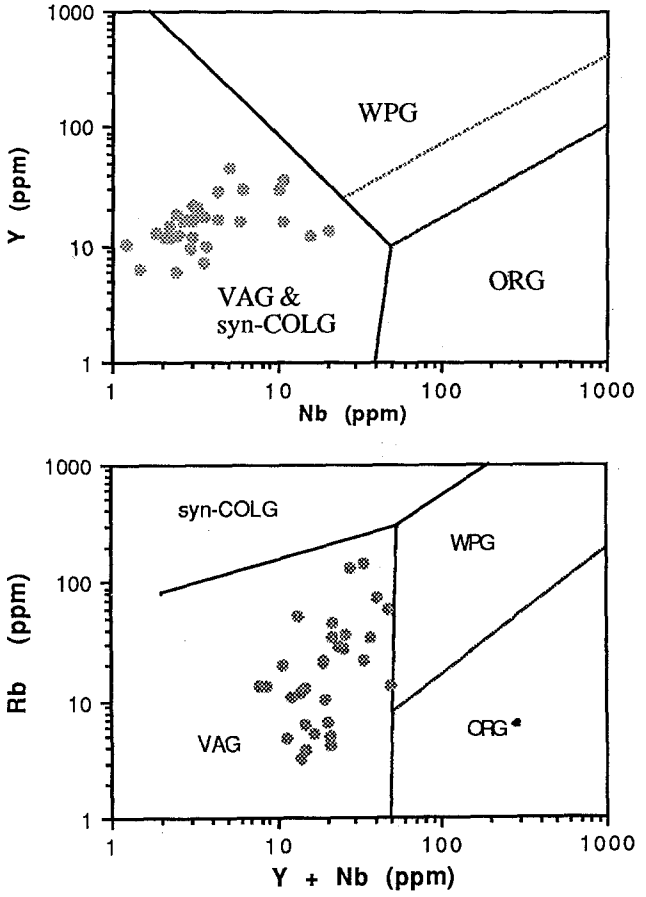

Fig. 5. Discrimination diagrams after Pearce et al. (1984) showing fields of various geodynamic settings for granitic rocks and position of Hafafit samples (based on Table 1). VAG = Volcanic arc granites; COLG = collisional granites; WPG = within-plate granites; and ORG = orogenic granites

Abdel-Khalek et al. (1992) recognized muscovite-biotite granodiorite gneiss and biotite granodiorite gneiss, the latter alternating with thin layers of hornblende biotite and garnet biotite gneisses, all derived from granodioritic precursors. Metatectic rocks are restricted to occurrences of granitic orthogneiss and frequently show gradational contacts with these rocks. *In situ* anatexis occurs in a number of localities within the migmatite terrain and was documented in detail by Stietzel (1987). The amphibolites are associated with the hornblende gneisses and may originally have been mafic dykes or basaltic flows. In view of the lack of radiometric data, Stietzel (1987) was unable to assign the gneiss terrain to either a pre-Pan-African infrastructure or to a strongly deformed Pan-African calc-alkaline intrusive suite, but in any case he considered it to predate the Pan-African ophiolitic mélange with which the gneisses are in tectonic contact. Abdel-Khalek et al. (1992) concluded the gneisses to represent an autochthonous infrastructure and that the ophiolitic mélange was thrust over them during plate convergence. They also considered the gneisses ('old gneisses' in their terminology) to predate the 'Older Granites' of Hussein et al. (1982). Our sample EG 747 is representative of the widespread, grey quartzofeldspathic (granitic to granodioritic) gneisses with migmatitic schlieren which are exposed in Wadi Bitan and its tributaries.

The gneisses of Wadi Feiran in Sinai consist of a variety of lithologies such as biotite hornblende gneiss, calc-silicate gneiss and quartzofeldsphatic gneiss, which El-Gaby and Ahmed (1980) interpreted to represent a thick sedimentary succession, locally metamorphosed to granulite grade. We did not observe any granulites in this terrain, and consider these rocks to have experienced amphibolite facies regional metamorphism. In contrast with El-Gaby and Ahmed (1980) and Stern and Manton (1987), we interpret the quartzofeldsphatic gneisses as strongly deformed granitoids and our sample EG 772, which is a strongly foliated diorite, was taken from this lithology, very close to the location sampled by Stern and Manton (1987). These workers dated one fraction of small, euhedral zircons from a sample of quartzofeldspathic gneiss and obtained a $^{207}Pb/^{206}Pb$ age of 632 ± 3 Ma, whereas zircons from a strongly foliated granodiorite in parallel tectonic contact with the quartzofeldspathic gneisses yielded an age of 782 ± 7 Ma. This latter granodiorite constitutes a distinct igneous body which cuts the foliation in the older dioritic gneisses sampled by us.

Single zircon evaporation

Kober (1986) has shown that the radiogenic Pb components with the highest activation energy normally occur in the undamaged crystalline zircon phase that shows no post-crystallization Pb loss and therefore yields concordant $^{207}Pb/^{206}Pb$ ages. Pb phases in zircon affected by radiation damage or by unmixing (metamict zones) have a low activation energy and are removed during low temperature evaporation. The method involves repeated evaporation and deposition of Pb from chemically untreated single zircons (Kober, 1987) until no further changes in the measured $^{207}Pb/^{206}Pb$ ratios are observed. The evaporation technique has since been shown to provide precise and reliable ages, even for zircons from metamorphic terrains, and the technique has been widely used in the study of igneous and metamorphic rocks (Kober et al., 1989; Kröner et al., 1991; 1993; Cocherie et al., 1992). However, in rare cases where severe Pb loss during granulite metamorphism affected the isotopic composition of the *entire* zircon grain, the method produces variable apparent $^{207}Pb/^{206}Pb$ ages which reflect the Pb loss pattern and are usually significantly lower than the true age of crystallization (e.g. Kröner and Williams, 1993; Kröner et al., 1993).

Isotopic measurements were carried out on a Finnigan-MAT 261 mass spectrometer in the Max-Planck-Institut für Chemie in Mainz. Details of the analytical procedure are given in Kröner et al. (1991). The ratio $^{206}Pb/^{204}Pb$ monitors the common lead component and, where necessary, a correction was made using the model of Stacey and

Table 2. Isotopic data from single grain zircon evaporation

Sample Number	Grain	Morphology	Mass scans*	Evaporation temperature (°C)	Mean $^{207}Pb/^{206}Pb$ ratio** and 1σ error	$^{207}Pb/^{206}Pb$ age and 1σ error
EG 27	1	Long, euhedral	82	1580	0.06275 ± 38	700 ± 13
	2		82	1590	0.06275 ± 35	700 ± 12
	1, 2		164		0.06275 ± 35	700 ± 12
EG 28	1	Long, clear,	42	1590	0.06275 ± 49	700 ± 16
	2	euhedral	58	1580	0.06266 ± 23	697 ± 8
	3		73	1555	0.06272 ± 48	699 ± 16
	1–3		173		0.06271 ± 41	698 ± 14
EG 30	1	As above	50	1570	0.06204 ± 28	675 ± 9
	2		56	1580	0.06210 ± 27	678 ± 9
	1, 2		106		0.06207 ± 28	677 ± 9
EG 747	1	Long, euhedral,	33	1580	0.06286 ± 25	704 ± 8
	2	yellow–brown,	83	1590	0.06287 ± 23	704 ± 8
	3	ends rounded	59	1580	0.06286 ± 21	704 ± 7
	1–3		175		0.06286 ± 23	704 ± 8
EG 772	1	Long, clear,	64	1560	0.06567 ± 10	796 ± 3
	2	euhedral	71	1540	0.06569 ± 13	796 ± 4
	3		50	1575	0.06567 ± 20	796 ± 6
	4		66	1575	0.06567 ± 26	796 ± 13
	5		149	1598	0.06567 ± 24	796 ± 9
	1–5				0.06567 ± 19	796 ± 6

* Number of $^{207}Pb/^{206}Pb$ ratios evaluated for age assessment.
** Observed mean ratio corrected for non-radiogenic Pb where necessary. Errors based on uncertainties in counting statistics.

Kramers (1975). No correction was made for mass fractionation which is of the order of 1‰ (Kober, 1987), significantly less than the relative standard deviation of the measured $^{207}Pb/^{206}Pb$ ratios (see Table 2) and insignificant at the age range considered in this study. The calculated ages and uncertainties are based on the means of all ratios evaluated and their 1-σ errors after the Dixon test (Dixon, 1950) was used as an outlier test in the statistical assessment of the measured values.

In our experiments evaporation temperatures were gradually increased in 20–30 °C steps during repeated evaporation–deposition cycles until no further changes in the $^{207}Pb/^{206}Pb$ ratios were observed. Only data from the high temperature runs or those with no changes in the Pb isotope ratios were considered for geochronological evaluation. In most cases no significant change in the $^{207}Pb/^{206}Pb$ ratio was recorded on progressive heating, a feature suggesting that most zircons analysed contained only one stable radiogenic lead phase. The calculated ages and uncertainties are based on the means of all ratios evaluated and their 1-σ errors and are presented in Table 2. The $^{207}Pb/^{206}Pb$ spectra are shown in histograms that allow visual assessment of the data distribution from which the ages are derived. Wherever possible, several grains were analysed from each sample and the mean $^{207}Pb/^{206}Pb$ age calculated from the combined isotopic ratios of these separate measurements (Table 2) is considered to most closely reflect the original magmatic crystallization age of the zircons evaporated.

Zircon ages

Samples EG 27 and 28 are trondhjemites, whereas sample EG30 is a granite (see Table 1). Field relationships clearly show EG 27 to be the oldest, intruded by material represented by sample EG 28. EG 30, in turn, represents material intrusive into the trondhjemite of EG 28. Sample EG 27 comes from just outside the largest gneiss culmination at Hafafit, whereas samples EG 28 and 30 were collected inside the dome (Fig. 1).

The zircons of all three samples are clear, long-prismatic and euhedral without cores or inclusions. Magmatic zonation can occasionally be observed with reflected light under a binocular microscope. There is no doubt that these zircons are exclusively of igneous origin. Two grains from sample EG 27 were evaporated individually and yielded uniform $^{207}Pb/^{206}Pb$ ratios (Table 2, Fig. 6a), which combine to a mean age of 700 ± 12 Ma. This is interpreted to reflect the time of emplacement of the trondhjemitic gneiss protolith. Three grains evaporated from sample EG 28 yielded a mean age of 698 ± 14 Ma (Table 2, Fig. 6b), which is statistically indistinguishable from that of EG 27 and suggests that the two units were emplaced within a short period of time not resolvable by our zircon geochronology. The results also demonstrate that the trondhjemitic gneisses inside and outside the domal culminations belong to the same intrusive event.

Two zircons from granite gneiss sample EG 30 yielded a mean $^{207}Pb/^{206}Pb$ age of 677 ± 9 Ma (Table 2, Fig. 7),

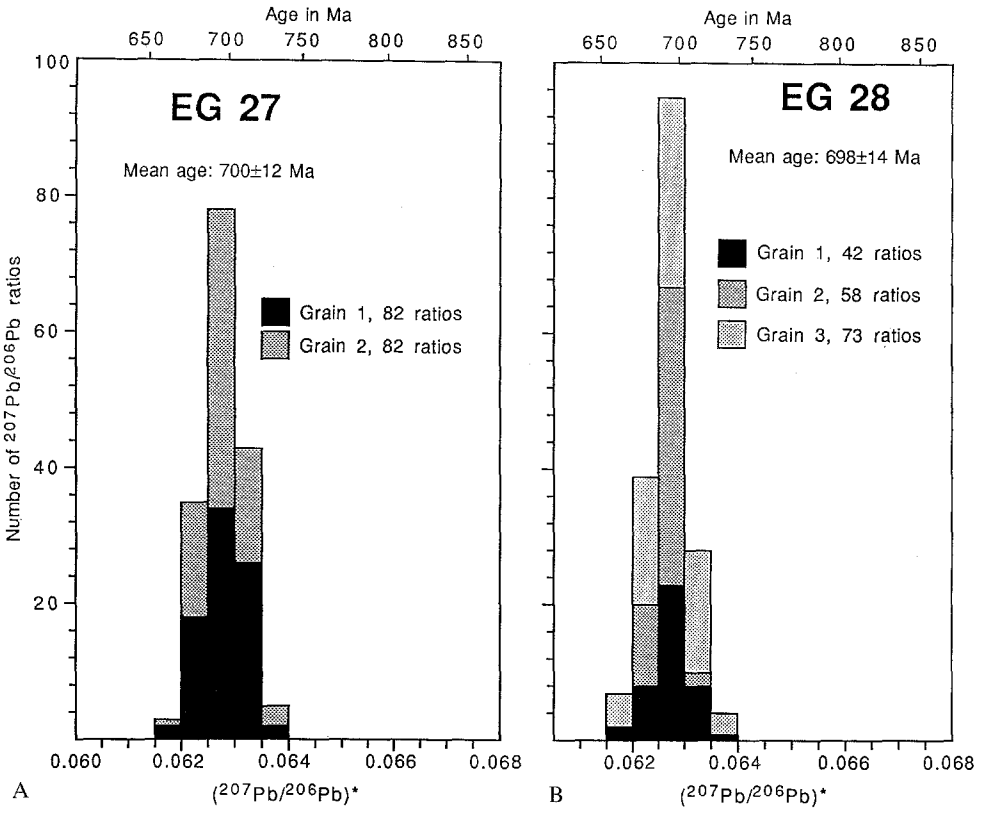

Fig. 6A, B. Histograms showing distribution of radiogenic lead isotope ratios derived from evaporation of single zircons from two trondhjemitic gneisses, Hafafit area, south Eastern Desert of Egypt. **A** Spectrum for two grains from sample EG 27, integrated from 164 ratios. **B** Spectrum for three grains from sample EG 28, integrated from 173 ratios. Mean ages are given with standard errors

distinctly younger than the ages derived from the two trondhjemitic gneisses and suggesting that the granite protolith of this gneiss was emplaced about 20 Ma after the trondhjemites. The combined data, although limited to three samples, suggest that the calc-alkaline granitoids at Hafafit were generated over a period of about 20 Ma. The $^{207}Pb/^{206}Pb$ zircon age of 682 Ma reported by Stern and Hedge (1985) for a sample from the northernmost dome structure is indistinguishable from our data. The low Sr initial ratio of 0.702 4 reported by Stern and Hedge (1985) and the fact that no zircon xenocrysts were detected in the samples analysed by us strongly support the conclusion that the Hafafit gneisses belong to a juvenile I-type suite of granitoids and were not derived from the melting of older crust.

It is likely that the granitoid gneisses and associated gabbroic rocks exposed in the domal structures at Hafafit belong to the suite of Shaitian or 'Older' granites which are widespread in the southern part of the ED. In this instance our data record a period of granitoid activity for this suite extending from ≈ 750 to ≈ 680 Ma as also found by Stern and Hedge (1985) for deformed granitoid rocks elsewhere in the southern ED. This plutonism reflects a period of magmatic arc formation which is virtually coeval with the formation of oceanic crust nearby, as represented by the Wadi Ghadir ophiolite dated at 745 $\pm$ 25 Ma (Kröner et al., 1992).

Three long, euhedral and yellow – brown zircons from granitic gneiss sample EG 747 of the Wadi Bitan gneiss terrain yielded a mean age of 704 $\pm$ 8 Ma (Table 2, Fig. 8) which we interpret as the magmatic emplacement age of the gneiss precursor. This is surprisingly similar to the ages from the Hafafit region and suggests that the Wadi Bitan granitoid gneisses also originated from the the ubiquitous suite of 'Older Granites' in the ED and do not represent a pre-Pan-African infrastructure as inferred by Abdel-Khalek et al. (1992). In view of this relatively young age there is also no need to infer the gneiss terrain to be autochthonous, and we consider it likely that the Wadi Bitanm gneisses represent similar thrust sheets as the gneisses at Hafafit, Meatiq and in the Wadi Allaqi area (Ries et al., 1983; Wallbrecher et al. 1993, Greiling et al., in press).

Lastly, five long, clear, euhedral zircons from Wadi Feiran gneiss sample EG 772 of south-west Sinai have very uniform $^{207}Pb/^{206}Pb$ ratios (Table 2) which combine to a mean age of 796 $\pm$ 6 Ma (Fig. 9). The zircon morphology and uniform isotopic composition convincingly demonstrate that sample EG 772 represents a granitoid orthogneiss and we therefore interpret this age as closely approximating the time of magmatic emplacement. Our age is slightly higher than the date of 782 $\pm$ 7 Ma for a granodioritic gneiss analysed by Stern and Manton (1987), and this is in line with our field observation that the granodiorite intrudes already foliated diorite. The fabric-forming event in the dioritic gneiss is therefore bracketed by the two ages above, and our results reiterate the conclusions of Stern and Manton (1987) that the Wadi Feiran suite is part of the Pan-African assemblage.

The age of 796 $\pm$ 6 Ma for the Feiran gneiss is virtually identical to the timing of felsic volcanic and intrusive

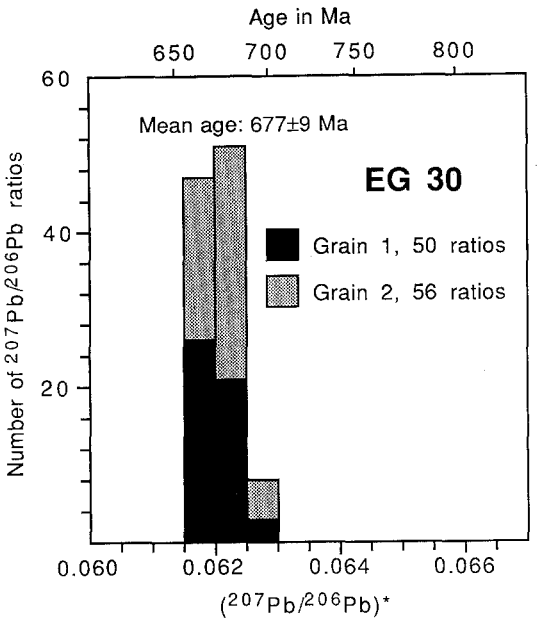

Fig. 7. Histogram showing distribution of radiogenic lead isotope ratios derived from evaporation of two zircon grains from granitic gneiss sample EG 30, Hafafit area, south Eastern Desert of Egypt. The spectrum plotted has been integrated from 106 ratios. Mean age is given with standard error

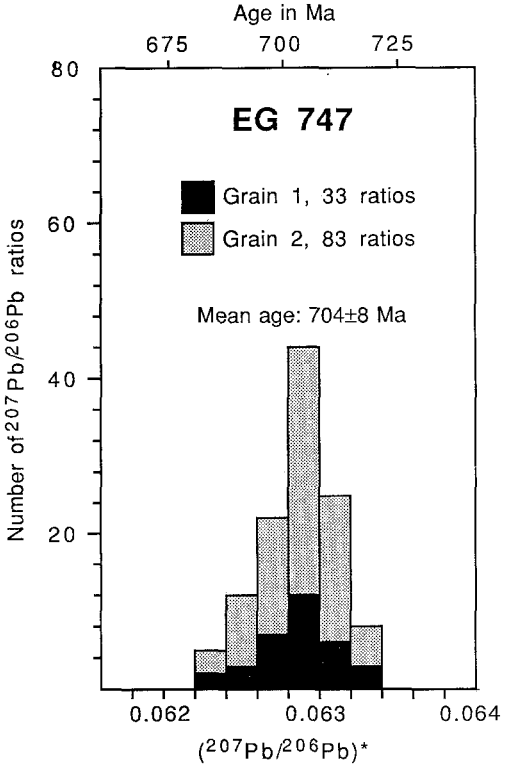

Fig. 8. Histogram showing distribution of radiogenic lead isotope ratios derived from evaporation of two zircon grains from migmatitic granitic gneiss sample EG 747, Wadi Bitan, south Eastern Desert of Egypt. The spectrum plotted has been integrated from 116 ratios. Mean age is given with standard error

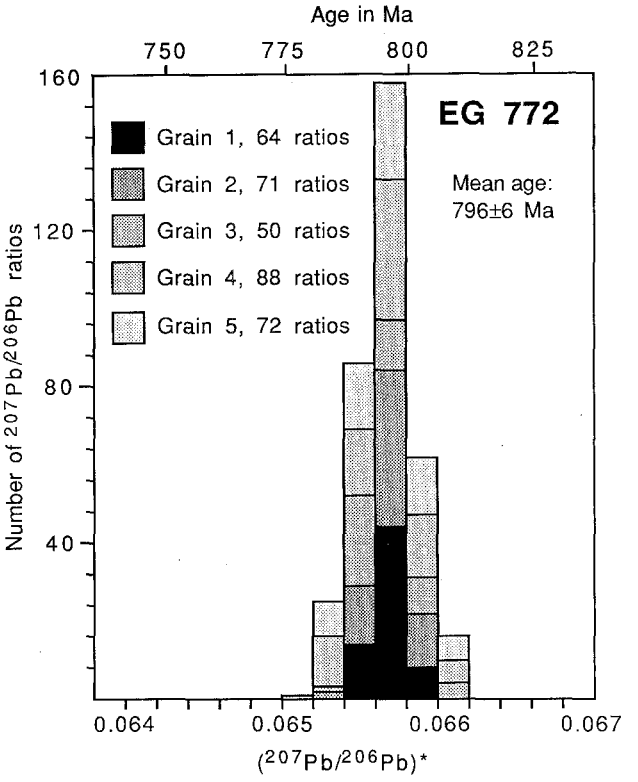

Fig. 9. Histogram showing distribution of radiogenic lead isotope ratios derived from evaporation of five zircon grains from granitic gneiss sample EG 747, Wadi Feiran, Sinai. The spectrum plotted has been integrated from 348 ratios. Mean age is given with standard error

activity associated with island-arc formation in north-east Sinai and around Elat in southern Israel (Kröner et al., 1990) and suggests that this event has affected virtually the entire terrain of the Sinai Peninsula.

Conclusions

Our zircon ages confirm that granitoid gneisses exposed in the southern ED and in south-west Sinai and which have previously been considered to represent an ancient basement are, in fact, of Pan-African age and were probably generated during magmatic arc evolution without involvement of older continental crust. This conclusion reiterates previous suggestions by Harris et al. (1983), Stern and Hedge (1985), Stern and Manton (1987) and Kröner et al. (1990). The apparently complex nature of these rocks was brought about by intense post-emplacement deformation and accompanying metamorphism, which locally led to the formation of migmatites such as at Hafafit and in the Wadi Bitan area.

These examples demonstrate that it is dangerous, and often incorrect, to postulate relative age differences in different rock units solely on the basis of differences in the degree of deformation and metamorphism, and our data support the general concept of a tectonostratigraphy in

the ED (Bennett and Mosley, 1987; Greiling et al., in press) with no evidence for an autochthonous basement.

Acknowledgements This research was part of a collaborative project between Mainz University and the Egyptian Geological Survey and Mining Authority funded by the Deutsche Forschungsgemeinschaft (DFG) and the German Ministry of Technology (BMfT) through KFA Jülich. We thank A. W. Hofmann for analytical facilities at the Max-Planck Institut für Chemie in Mainz and R. J. Stern and R. O. Greiling for constructive comments on the manuscript.

References

Abdel-Khalek, ML, Takla MA, Sehim A, Hamini Z, El Manawi AW (1992) Geology and tectonic evolution of Wadi Beitan area, Southeastern Desert, Egypt. In: Sadek A (ed) Geology of the Arab World. Cairo University, pp 369–394

Abdel-Monem AA, Hurley PM (1979) U–Pb dating of zircons from psammitic gneisses, Wadi Abu Rusheid-Wadi Sikait area, Egypt. Inst Appl Geol King Abdulaziz Univ Jeddah, Bull 3: 165–170

Abdel-Rahman AFM, Martin RF (1987) Late Pan-African magmatism and crustal development in northeastern Egypt. Geol 22: 281–301

Barker F, Arth JG, Hudson T (1981) Tonalites in crustal evolution. Phil Trans R Soc London A 301: 293–303

Bennett, JD, Mosley PN (1987) Tiered-tectonics and evolution, Eastern Desert and Sinai. In: Matheis G, Schandelmeier H (eds) Current Research in African Earth Sciences. Balkema, Rotterdam, pp 79–82

Chappell BW, White AJR (1974) Two contrasting granite types. Pacific Geol 8: 173–174

Cocherie A, Guerrot C, Rossi PH (1992) Single-zircon dating by step-wise Pb evaporation: comparison with other geochronological techniques applied to the Hercynian granites of Corsica, france. Chem Geol (Isotope Geosci Sect) 101: 131–141

Dixon TH (1981) Age and chemical characteristics of some pre-Pan-African rocks in the Egyptian shield. Precambrian Res 14: 119–133

Dixon, WJ (1950) Analyses of extreme values. Ann Math Statis 21: 488–506

El-Gaby S, Ahmed AA (1980) The Feiran-Solaf gneiss belt, SW Sinai, Egypt. Inst Appl Geol King Abdulaziz Univ Jeddah Bull 3 (4): 95–105

El-Gaby S, El-Nady O, Khudeir A (1984) The tectonic evolution of the basement complex in the central Eastern Desert of Egypt. Geol Rundsch 73: 1019–1036

El-Gaby S, List FK, Tehrani R (1988) Geology, evolution and metallogenesis of the Pan-African belt in Egypt. In: El-Gaby S, Greiling RO (eds) The Pan-African Belt of Northeast Africa and Adjacent Areas. Viehweg-Verlag, Wiesbaden, pp 17–68

El Gaby S, List FK, Tehrani R (1990) The basement complex of the Eastern Desert and Sinai. In: Said R (ed) The Geology of Egypt. Balkema, Rotterdam, pp 175–184

El Kaliuobi BA, El Ramly MF (1991) Nomenclature, origin and tectonic setup of the "granite" suite at Wadi Shait, South Eastern Desert, Egypt. Ann Geol Surv Egypt 17: 1–17

El-Ramly MF (1972) A new geological map for the basement rocks in the Eastern and Southwestern Desert of Egypt. Ann Geol Surv Egypt 2: 1–18

El-Ramly MF, Akaad MK (1960) The basement complex in the CED of Egypt between lat. 24°30′ and 25°40′. Geol Surv Egypt Pap No 8: 33 pp

El-Ramly MF, Roufaiel GSS (1974) Sodic-silica metasomatism and introduced zircon in the Migif-Hafafit gneisses, Eastern Desert. Egypt J Geol 18: 119–126

El-Ramly MF, Greiling RO, Kröner A, Rashwan AAA (1984) On the tectonic evolution of the Wadi Hafafit area and environs, Eastern Desert of Egypt. Fac Sci King Abdulaziz Univ Jeddah Bull 6: 113–126

Geological Map of Egypt Scale 1 : 2 000 000 (1981) Egyptian Geological Survey and Mining Authority, Cairo

Greiling RO, El-Ramly MF (1990) Wadi Hafafit area – structural geology – Egypt. Geological Map 1 : 100 000. Technische Fachhochschule, Berlin

Greiling R, Kröner A, El-Ramly MF (1984) Structural interference patterns and their origin in the Pan-African basement of the southeastern Desert of Egypt. In: Kröner A, Greiling R (eds) Precambrian Tectonics Illustrated. E. Schweizerbart'sche Verlagsbuchhandlung, Stuttgart, pp 401–412

Greiling RO, Kröner A, El-Ramly MF, Rashwan AA (1988) Structural relationships between the southern and central parts of the Eastern Desert of Egypt: details of a fold and thrust belt. In: El-Gaby S, Greiling RO (eds) The Pan-African Belt of Northeast Africa and Adjacent Areas. Vieweg Verlag, Braunschweig/Wiesbaden, pp 121–146

Greiling RO, Abdeen MM, Dardir AA, El Akhal H, El Ramly MF, Kamal El Din GM, Osman AF, Rashwan AA, Rice AHN, Sadek MF. A structural synthesis of the late Proterozoic Nubian shield in Egypt. Geol Rundsch 83: 484–501

Habib MS, Ahmed AA, El-Nady OM (1985) Two orogenies in the Meatiq area of the CED, Egypt. Precambrian Res 30: 83–111

Harris NBW, Hawkesworth CJ, Ries AC (1984) Crustal evolution in northeast and east Africa from model Nd ages. Nature 309: 773–776

Harris NBW, Gass IG, Hawkesworth CJ (1990) A geochemical approach to allochthonous terranes: a Pan-African case study. Phil Trans R Soc London A 331: 533–548

Hussein AA, Ali MM, El-Ramly MF (1982) A proposed new classification of the granites of Egypt. J Volcanol Geothermal Res 14: 187–198

Kober B (1986) Whole-grain evaporation for $^{207}Pb/^{206}Pb$-age-investigations on single zircons using a double-filament thermal ion source. Contrib Mineral Petrol 93: 482–490

Kober B (1987) Single-zircon evaporation combined with Pb^+ emitter-bedding for $^{207}Pb/^{206}Pb$-age investigations using thermal ion mass spectrometry, and implications to zirconology. Contrib Mineral Petrol 96: 63–71

Kober B, Pidgeon RT, Lippolt HJ (1989) Single-zircon dating by stepwise Pb-evaporation constrains the Archaean history of detrital zircons from the Jack Hills, Western Australia. Earth Planet Sci Lett 91: 286–296

Kröner A (1979) Pan African plate tectonics and its repercussions on the crust of northeast Africa. Geol Rundsch 68: 565–583

Kröner A, Williams IS (1993) Age of metamorphism in the high-grade rocks of Sri Lanka. J Geol 101: 513–521

Kröner A, Greiling RO, Reischmann T, Hussein IM, Stern RJ, Dürr S, Krüger J, Zimmer M (1987) Pan-African crustal evolution in the Nubian segment of northeast Africa. In: Kröner A (ed) Proterozoic Lithospheric Evolution. Am. Geophys Union, Geodyn Ser 17: 235–257

Kröner A, Reischmann T, Wust HJ, Rashwan AA (1988) Is there any pre-Pan-African basement in the Eastern Desert of Egypt? In: El-Gaby S, Greiling RO (ed) The Pan-African Belt of Northeast Africa and Adjacent Areas. Vieweg Verlag, Braunschweig/Wiesbaden: 95–120

Kröner A, Eyal M, Eyal Y (1990) Early Pan-African evolution of the basement around Elat, Israel, and the Sinai Peninsula revealed by single-zircon evaporation dating, and implication for crustal accretion rates. Geology 18: 545–548

Kröner A, Byerly GR, Lowe DR (1991) Chronology of early Archaean granite-greenstone evolution in the Barberton Mountain Land, South Africa, based on precise dating by single zircon evaporation. Earth Planet Sci Lett 103: 41–54

Kröner A, Todt W, Hussein IM, Mansour M, Rashwan AAA (1992) Dating of late Proterozoic ophiolites in Egypt and the Sudan using

the single zircon evaporation technique. Precambrian Res 59: 15–32

Kröner A, Jaeckel P, Williams IS (1993) Pb-loss patterns in zircons from a high-grade metamorphic terrain as revealed by different dating methods: U–Pb and Pb–Pb ages for igneous and metamorphic zircons from northern Sri Lanka. Precambrian Res 66: 151–181

Pearce JA, Gale GH (1977) Identification of ore-deposition environment from trace element geochemistry of associated igneous host rocks. Geol Soc Lond, Spec Publ 7, 14–24

Pearce JA, Harris NBW, Tindle AG (1984) Trace element discrimination diagrams for the tectonic interpretation of granitic rocks. Petrol 25: 956–983

Rashwan AA (1991) Petrography, geochemistry and petrogenesis of the Migif-Hafafit gneisses at Hafafit Mine area, Egypt. Forschungszentrum Jülich, Sci Ser Int Bur 5: 359 pp

Ries AC, Shackleton RM, Graham RH, Fitches WR (1983) Pan-African structure, ophiolites and mélange in the Eastern Desert of Egypt: a traverse at 26°N. J Geol Soc London 140: 75–95

Schandelmeier H, Darbyshire DPF, Harns U, Richter A (1988) The East Saharan Craton: evidence for pre-Pan-African crust in NE Africa West of the Nile. In: El-Gaby S, Greiling RO (eds) The Pan-African Belt of Northeast Africa and Adjacent Areas. Vieweg Verlag, Braunschweig/Wiesbaden: 69–94

Schmidt DL, Brown GF (1984) Major-element chemical evolution of the late Proterozoic shield of Saudi Arabia. Fac Earth Sci, King Abdulaziz Univ Jeddah Bull 6: 1–21

Schürmann HME (1966) The Precambrian Along the Gulf of Suez and the Northern Part of the Red Sea. Brill, Leiden 404 pp

Shimron AE (1980) Proterozoic island arc volcanism and sedimentation in Sinai. Precambrian Res 12: 437–458

Stacey JS, Kramers JD (1975) Approximation of terrestrial lead isotope evolution by a two-stage model. Earth Planet Sci Lett 26: 207–221

Stern RJ, Hedge CE (1985) Geochronologic and isotopic constraints on late Precambrian crustal evolution in the Eastern Desert of Egypt. Am J Sci 285: 97–127

Stern RJ, Kröner A (1993) Late Precambrian crustal evolution in NE Sudan: isotopic and geochronologic constraints. J Geol 101: 555–574

Stern RJ, Manton WI (1987) Age of Feiran basement rocks, Sinai: implications for late Precambrian crustal evolution in the northern Arabian–Nubian shield. J Geol Soc Lond 144: 569–575

Stern RJ, Kröner A, Manton WI, Reischmann T, Mansour M, Hussein IM (1989) Geochronology of the late Precambrian Hamisana shear zone, Red Sea Hills, Sudan and Egypt. J Geol Soc London 146: 1017–1029

Stietzel HJ (1987) Geologie und Petrographie der Granite und Metamorphite im Gebiet des Wadi Hodein, SE-Ägypten – Geländeuntersuchungen und Fernerkundung. Berliner Geowiss Abh (A) 90: 121 pp

Sturchio NC, Sultan M, Batiza R (1983) Geology and origin of Meatiq Dome, Egypt: a Precambrian metamorphic core complex? Geology 11: 72–76

Sturchio NC, Sultan M, Sylvester P, Batiza R, Hedge C, El Shazly EM, Bdel-Maguid A (1994) Geology, age, and origin of the Meatiq dome: implications for the Precambrian stratigraphy and tectonic evolution of the eastern desert of Egypt. Fac Earth Sci, King Abdulaziz Univ Jeddah Bull 6: 127–143

Therani R, El-Gaby S, List FK, Meissner B (1988) Geological Map of Egypt 1:250000, Sheet Gebel Hamata. Technische Fachhochschule, Berlin

Wallbrecher E, Fritz H, Khudeir AA, Farahad F (1993) Kinematics of Panafrican thrusting and extension in Egypt. In: Thorweihe U, Schandelmeier H (eds) Geoscientific Research in NE Africa. Balkema, Rotterdam, pp 27–30

Watson EB (1979) Zircon saturation in felsic liquids: experimental results and applications to trace element geochemistry. Contrib Mineral Petrol 70: 407–419